

Major and Trace element geochemistry of Bay of Bengal Sediments: Implications to Provenances and their controlling factors

Gyana Ranjan Tripathy^{1,2,*}, Sunil Kumar Singh¹ and V Ramaswamy²

¹Geosciences Division, Physical Research Laboratory, Ahmedabad-380009, India

²National Institute of Oceanography, Dona Paula, Goa-403004, India

*Corresponding Author: grtripathy@gmail.com

Keywords: Bay of Bengal sediments; Geochemistry; Provenances; Himalaya; Deccan traps; climate.

Abstract

Major and trace elements of sediments from a ~13-m long piston core (SK187/PC33) from the western Bay of Bengal have been investigated in this study to infer about the changes in provenances and related controlling factors during the last glacial-interglacial period. Factor analysis of these geochemical dataset ascertains dominant role of riverine supply of sediments in regulating the geochemistry of SK187/PC33 sediments. The Al-normalized major (K and Ti) and trace elemental (Cu and Cr) ratios of these marine sediments fall within the ranges observed for their major provenances, *viz.* Ganga, Brahmaputra and the Godavari-Krishna (GK) rivers and depth profiles of these ratios showed significant variations with synchronous excursion at around the last glacial maxima (LGM), implying a change in their provenances with relatively reduced Himalayan contribution during this climatic event. Relatively higher CIA and Ti/Ca ratios with lower K/Al ratios of these sediments during the Holocene hint intense chemical weathering in the river basins in response to strengthened monsoon during this period. Inverse model calculation of Al-normalized elemental ratios of the sediments estimated an average sediment contribution of $66 \pm 13\%$ and $34 \pm 13\%$ from the Himalayan and the peninsular Indian rivers to the core site respectively. Consistent with the depth profiles of elemental ratios, the estimated sediment contributions from the Himalayan rivers are observed to decrease by ~20% from the Himalayan rivers, particularly that of the Ganga, to the studied location during the LGM. Lowering of sediment supply from the Himalaya (Ganga) during the LGM is due to weakening of south-west monsoon and reduction in available exposure area for weathering due to extent of glacier cover. Outcomes of this study underscore the strong linkage between erosion and climate.

1. Introduction

Sediments of the western Bay of Bengal (BoB) are supplied mainly by the major rivers draining the Himalayas (*e.g.* the Brahmaputra and the Ganga) and the peninsular India (*e.g.* the Godavari, Krishna and the Mahanadi). Presently, these rivers together supply about 1350 million tons of sediments per year to the BoB, which accounts for ~8% of the total riverine supply to the oceans (Milliman and Syvitski, 1992; Milliman, 2001). This sediment load is disproportionately (~5 times) higher compared to the fraction of areal coverage of these rivers to the global drainage area underscoring the important role of physical erosion in these river basins on the global sedimentary budget. Further, the erosion patterns of these river basins and their spatio-temporal variations have received significant attention due to their key role in the global carbon budget (France-Lanord et al., 1993; Galy and France-Lanord, 2001; Clift et al., 2008; Pattan et al., 2008; Singh et al., 2008; Rahaman et al., 2009; Krishnaswami and Tripathy, 2012). Researches based on sediment flux and their chemical and isotopic properties have demonstrated that the ongoing physical erosion in these river basins is by and large regulated by climate (rainfall) over millennium time scale (Islam et al., 1999; Singh and France-Lanord, 2002; Goodbred, 2003; Singh et al., 2008; Chakrapani and Saini, 2009; Panda et al., 2011). It has also been documented that the climate over this region has varied appreciably over ka time scale (Duplessey, 1982; Prell and Kutzbach, 1987; Sarkar et al., 1990; Tiwari et al., 2005). It is therefore, expected that physical erosion pattern over these river basins could also have varied in the past in response to these climate changes. Sediments archived in the western BoB can provide useful information on the palaeo-erosion pattern of these river basins and therefore on climate-erosion link, which continues to be a topic of debate.

Existing studies on the reconstruction of erosion pattern of river basins from the Himalaya and the peninsular India during last few tens of ka have led to diverging views. Temporal variations in the sedimentological and Sr-Nd isotopic properties of the BoB sediments indicated relative changes in the supply of sediments from different sources which in turn have been attributed to variability in monsoon intensity in the past (Ahmad et al., 2005; Kessarkar et al., 2005). Prakashbabu et al. (2010), based on down-core variations in the granulometric, geochemical and mineral magnetism in a core from the eastern BoB observed a shift in sediment provenance from the Brahmaputra to the Ganga since early Holocene which has been attributed to climatic changes. More recently, Sr-Nd isotopic study of the Bay of Bengal sediments by Tripathy et al. (2011a) observed reduced sediment supply from the Himalaya to the western BoB during last glacial maximum (LGM) due to weakening of south-west monsoon (Prell

and Kutzbach, 1987) and larger glacier cover over the Higher Himalaya (HH) (Owen et al., 2002); all these studies providing additional support for the climate-erosion link. The hypothesis of climate-erosion link was further strengthened by the studies of Clift et al. (2008) and Rahaman et al. (2009), both of which showed varying erosion rate over the Higher and the Lesser Himalaya in response to climatic changes during last tens of ka. In contrast to these results, there are also lines of evidence that suggest lack of major changes in sediment provenance during climatic events, challenging the climate-erosion relation. For example, Colin et al. (1999) and Galy et al. (2008) based on Sr-Nd isotopic composition of BoB sediments showed no systematic change in sediment source despite changes in climate. Similar studies on tracking provenances of sediments from the Eastern Arabian Sea also have not indicated any major changes in supply from the peninsular Indian river basins over a ka time scale (Kessarkar et al., 2003; Goswami et al., 2012). In order to evaluate the impact of climate change on the erosion patterns of the Himalaya and peninsular Indian river basins, it would be interesting to compare the temporal variations in relative sediment contribution from these rivers to the western BoB.

Earlier studies on the provenances of BoB sediments relied mainly on their clay mineral and Sr-Nd isotopic composition. Prior to this, there have been a few studies on the chemical composition of BoB sediments (Sarin et al., 1979; Colin et al., 2006; Prakashbabu et al., 2010), which can provide useful information about both the chemical and physical erosion pattern of the river basins. The present study attempts to track the provenances of sediments from the western Bay of Bengal and to reconstruct the palaeo-erosion pattern of the river basins draining the Himalaya and peninsular India using down-core variations of their major and trace elemental composition. Further, this study employs an integrated approach of factor analysis and inverse modeling to quantitatively estimate the sediment contribution from various sources to the core site and their temporal variations. The results of this study on temporal variations in provenances are used to assess the role of climate in regulating the erosional pattern of the river basins of the Himalaya and peninsular India.

2. Material and Methods

The marine sediment analyzed in this study is from a ~13-m long piston core (SK187/PC33; Tripathy et al., 2011a) raised from the western BoB (Fig. 1; 16°16' N, 84° 30' E; Water depth: 3003 m) during the 187th expedition of ORV *Sagar Kanya*. This core was examined onboard for some of its physical properties (P-wave velocity, bulk density and gamma ray attenuation) using a Geotek® multi-

sensor core logger. These measurements indicate that the core is turbidite-free and preserves a continuous record of sedimentation. The core was sub-sampled at 1-2 cm interval and stored at the National Institute of Oceanography core repository. Chemical analysis and Sr-Nd isotopic composition of the sediments was carried out at an interval of ~50 cm, at the Physical Research Laboratory, Ahmedabad. Tripathy et al. (2011a) in an early study reported the depth-age model, magnetic susceptibility and Sr-Nd isotopic composition of these sediments. The present study is limited to major and trace element composition of the sediment core and its potential as a tool to reconstruct the palaeo-erosion pattern of the river basins supplying sediments to the core-site. The depth-age model for the SK187/PC33 was developed based on the ^{14}C ages of inorganic carbon (CaCO_3) and magnetic susceptibility stratigraphy. The ^{14}C depth-age model was developed after critically evaluating the impact of contribution from detrital carbonates (Tripathy et al., 2011a). This model suggests that sediments deposited in the interval 600-700 cmbsf corresponds to the LGM. The sedimentation rate of the core shows significant variation with depth, the rate is lower during the LGM (0.2 mm/yr) compared to that after this climatic event (2.7 mm/yr).

The sub-samples were powdered using an agate mortar, washed with de-ionized water to remove the sea-salts and ashed at 600°C to oxidize organic matters. The sea-salt and organic-matter free sediments were dissolved completely with repeated acid digestion using $\text{HF-HNO}_3\text{-HCl}$. These solutions of sediments were used to measure their major and trace elemental concentrations. Na and K were measured using Flame AAS, whereas the concentrations of other elements (Ca, Mg, Al, Fe, Ti, V, Ba, Cr, Sr, Mn, Cu, Co, Ni and Zn) were analyzed using ICP-AES (Jobin-Yvon, Ultima). Among these, the Al, Fe and V concentrations have already been reported by Tripathy et al. (2011a). Total carbon and nitrogen in the sediments (at ~10 cm interval) was analyzed using CN analyzer (FISON NA1500) using method of Bhushan et al., (2001), whereas carbonate content were determined using a CO_2 Coulometer (Model 5012, UIC Inc., Illinois, USA). Organic carbon was taken as difference between measured total carbon and inorganic carbon concentrations. A few samples were analyzed in replicate to determine the precision of measurements; these results yield for the coefficient of variation of about 5% or better for various elements. Major and trace element composition of USGS G-2 reference standard was also measured during the course of the study to check on the accuracy of analyses; this was found to be better than $\pm 10\%$ for most of the elements (Tripathy, 2011).

3. Results

3.1. Major and Trace elements

The concentrations of major and trace elements in sediments of the SK187/PC33 core are given in Table 1. The major elements, Na (0.54-2.39 wt%), K (1.03-3.08 wt%), Ca (0.74-29.37 wt%), Mg (0.80-3.39 wt%), Al (2.50-9.19 wt%), Fe (1.84-6.54 wt%), Ti (0.16-0.57 wt%) and Mn (0.03-1.09 wt%), show significant down-core variations. The average carbonate-free concentration of major elements (excluding Ca and Mn) in the core, as expected, is within the range of values (Table 2) reported for its possible sources, *viz.* the Ganga, Brahmaputra and the GK Rivers. The Ca concentration (6 ± 7 wt%) of the bulk sediments is higher compared to that reported for the Himalayan and the peninsular river sediments (Table 2) and is attributable to supply of CaCO_3 from biogenic sources. The carbonate-free concentrations of Mn, Sr and Ba are not calculated as these elements are known to be associated with carbonates in sea sediments. Carbonate-free concentrations of trace elements also fall within range of values reported for the Ganga, Brahmaputra and the GK sediments (Table 2), excluding Zn which seems to have marginally higher concentration in the SK187/PC33 sediments. This relatively higher Zn content and part of the variation in other elemental compositions of sediments can be attributed to change in their chemical composition due to size sorting during sediment transportation (Horowitz and Elrick, 1987; Bouchez et al., 2011) from their source to the Bay.

3.2. CaCO_3 , organic carbon (C_{org}) and total N content and C_{org}/N ratio

The concentrations of CaCO_3 , C_{org} , and total nitrogen, and C_{org}/N ratios with depth in the SK187/PC33 core are listed in Table 3. The carbonate content of the sediments shows a wide range from 0.2 to 53.9 wt% with majority of samples (97 out of 123) having <10 wt%. This temporal variation in the CaCO_3 (Fig. 3) is attributable to their relatively supply from detrital and biogenic carbonates. The mean CaCO_3 content for the SK187/PC33 sediments (~ 7 wt%) are higher compared to that of the sediments of the peninsular Indian rivers (~ 3 wt%; Das and Krishnaswami, 2007) and the Lower Meghna (~ 3 wt%; Galy and France-Lanord, 2001), combined flow of the Ganga and Brahmaputra river system in the Bangladesh. Two samples of SK187/PC33 (221-223 and 440-442 cm) have anomalously high CaCO_3 (~ 50 wt%). It is pertinent to mention here that the Sr and Nd isotopic compositions for these two samples also show anomalous signatures (Tripathy et al., 2011a) that hint at unique event of significant sediment supply.

The C_{org} and total nitrogen for these sediments range from 0.1 to 6.7 wt% and 0.01 to 0.4 wt% respectively. Except for three outliers, the samples have <2 wt% of C_{org} with an average of 0.8 ± 0.4 wt%, consistent with previously reported organic carbon content in BoB sediments (Galy et al., 2008). The average C_{org} concentration of the SK187/PC33 sediments is intermediate to those of the river sediments of Lower Meghna (0.6 wt%; Aucour et al., 2006) and Godavari (2.5 wt%; Gupta et al., 1997). The average total nitrogen content of the sediments analyzed in this study is 0.1 wt%. The C_{org}/N (atomic ratio) values of the sediments show a wide depth variation (1.1-26.3, excluding the two anomalous samples) with a mean value of 12 ± 4 . These measured parameters (carbonate, C_{org} , C_{org}/N), though exhibit depth variations; show no systematic evolution during last glacial-interglacial cycle (Fig. 2).

Comments: I don't really understand why you are comparing C.org percentage of PC33 with Meghna and Godavari sediments since PC33 gets additional organic matter from ocean productivity. Also better to use Total N in text and figures.

4. Discussions

4.1. Detrital component

The geochemistry of marine sediments is by and large an integration of its relative supply from the detrital, biogenic and hydrothermal sources. In order to employ geochemical composition of Bay of Bengal for reconstruction of palaeo-erosion pattern of near-by river basins, it is essential to establish that the major and trace elements are mainly from detrital sources. Towards this, the Al concentration of sediments can be used for reference as it behaves conservatively during chemical weathering of rocks and remains mostly immobile during chemical alterations. Support for the immobility of Al also comes from low dissolved Al ($\sim 0.1\%$) in the Himalayan rivers compared to its particulate flux (Lupker et al., 2012). Figure 3 shows the correlation of Al with other elements of sediments of SK187/PC33. Strong positive correlation of Al with most of the major and trace elements of SK187/PC33 sediments is observed (Fig. 3). The coefficient of correlations (r) between Al and other elemental abundances (Fig. 3) is observed to be statically significant (> 0.7) within 99% confidence interval. These r values though reduces marginally (> 0.6) after excluding two outliers (220-222 cm and 440-442 cm), but still remain to be statistically significant. This observation of strong co-relation between Al and other elements confirms that the geochemistry of sediments in the western BoB is mainly governed by their supply

from detrital sources and therefore, has the potential to provide information about changes in the sediment provenances in the past. Along with detrital supply, the correlation of Al with other chemical elements of the BoB sediments can also be due to size sorting of the sediments during erosion (Horowitz and Elrick, 1987; Bouchez et al., 2011). Therefore, the geochemistry of BoB sediments seems to be largely controlled by sediment sources and size sorting.

To assess the impact of chemical alteration of source rocks on the geochemistry of the SK187/PC33 sediments, their chemical index of alteration (CIA) was calculated. CIA provides information on the intensity of chemical weathering the sediments have undergone (Nesbitt and Young, 1982) and is defined as,

$$CIA = 100 \times \left(\frac{Al_2O_3}{Na_2O + K_2O + CaO^* + Al_2O_3} \right) \text{----- (1)}$$

where, all the elemental compositions are in molar units and the CaO* represents the silicate CaO concentrations in the sediments. CaO* is estimated by subtracting CaO content estimated using inorganic carbonates (assuming insignificant dolomite content in the BoB sediments) from the measured CaO of bulk sediments. All the samples, excluding the two outliers (220-222 cm (CIA: 37) and 440-442 cm (CIA: 21)), have CIA values between 41 and 77. The average CIA value for the BoB sediments is found to be 64 ± 13 . This average CIA value is similar to that reported for the Higher Himalaya (53 ± 7 ; Rai, 2008), and Lesser Himalaya (52 ± 7 ; Rai, 2008), but higher compared to that reported for the Deccan basalts (~ 37 (Range: 35-44); Das and Krishnaswami, 2007). To evaluate the impact of chemical weathering on the elemental ratios of the BoB sediments, CIA of the sediments is plotted against some of the key elemental ratios (particularly K/Al ($r^2=0.12$), Ti/Al ($r^2=0.09$), Cu/Al ($r^2=0.06$), Cr/Al ($r^2=0.00$); c.f. section 4.2 for application of these ratios) that can be used as a provenance indicator. The scatter plot of CIA with these elemental ratios (not shown) does not show any significant correlation, confirming that the chemical weathering have not altered the elemental ratios of the sediments and therefore, can be used to track their provenances and their relative contributions to the studied core location in the past.

4.1.1. Factor analysis

In order to better constrain the contributing factors towards the geochemistry of the SK187/PC33 sediments, factor analysis of the geochemical dataset (Table 1) have been carried out in this study. This analysis extracted four major factors (Table 4) having Eigen values greater than 1 and these factors can explain ~85% of the variance of the dataset. Among these four factors, the dominating factor (*Factor 1*) explains ~50% of the total variance and is primarily loaded with Al, Ti and Fe. Dominant loading of Al and Ti through *Factor 1* clearly implies this factor to represent the detrital source. This factor also characterized with higher loading for various trace elements (Ba, Cr, Co, Cu, Ni and V; Table 4) of the SK187/PC33 core, implying their dominant detrital supply. This inference is consistent with strong correlation of these trace elements with Al (Fig. 3). Higher loading of Fe in the *Factor 1* with weak loading for Mn ensures that Fe in these marine sediments is primarily of detrital origin. It is interesting to notice that insignificant amount of Fe and trace elements in the Bay of Bengal sediments are supplied through formation of Fe-Mn oxides, which an important geochemical process in the oceans particularly in the estuaries. This observation of minimal association of trace elements with the Fe-Mn oxides in the western Bay of Bengal is consistent with earlier reported insignificant correlation ($r = 0.17$) between Fe and Mn in the surface sediments from the Godavari-Krishna river shelf (Pattan et al., 2008). Along with detrital supply, the geochemistry of the BoB sediments are minutely also regulated by carbonates (*Factor 2*), and organic matters (*Factor 4*). It is unclear to assign a source for '*Factor 3*' which is primarily loaded with Zn, Mg and K (Table 4). One possible explanation for *Factor 3* could be their association with micro-nutrients that substitutes some of these elements in the marine sediments (Huang and Conte, 2009).

Factor analysis of the geochemical dataset for the SK187/PC33 core ascertains that most of these elements are primarily supplied *via* their detrital sources (Table 4). The location of SK187/PC33 core in the western BoB presently receives sediments mainly from the Ganga, Brahmaputra and the GK river system. The contemporary sediments of the Ganga river are dominantly derived from the Higher Himalaya with minor contribution from the Lesser Himalaya (Singh et al., 2008). Along with these provenances, the Brahmaputra river system also receives significant amount (~30%) of sediments from the Trans-Himalayan Batholith (TPB; Singh and France-Lanord, 2002). The sediments of the Godavari-Krishna river system are mainly derived from the geological units of its drainage basins, *viz.* Deccan Traps and Archean crust. The Deccan traps extend in about ~60% area of the Godavari drainage basin,

whereas it is ~20% of the drainage area of the Krishna river system (Subramanian et al., 2006). The chemical composition of the sediments from the SK187/PC33 must be therefore, controlled by the geochemistry of sources rocks from the HH, LH, TPB, Deccan traps and the Archean crust (Galy and France-Lanord, 2001; Singh and France-Lanord, 2002; Das and Krishnaswami, 2007; Braun et al., 2009). Figure 4 compares the geochemistry of SK187/PC33 sediments and its possible geological provenances in a $\text{Al}_2\text{O}_3\text{-CaO}^*\text{+Na}_2\text{O-K}_2\text{O}$ (A-CN-K) diagram. Most of the data for the sediments from the western BoB are well-bracketed by the chemical composition of their sediment sources (Fig. 4), implying that the geochemistry of the marine sediments preserves the signature of their sources. It is interesting to note here that some of the data fall towards the Al_2O_3 apex with higher values than that of the HH and LH, the major sediment supplier from the Himalaya to the Bay of Bengal. This observation could be attributable to size sorting of sediments during erosion (Horowitz and Elrick, 1987; Bouchez et al., 2011) where fine fractions of sediments are likely to have elevated concentrations of Al_2O_3 . The A-CN-K diagram therefore, points that the geochemical composition of the sediments is primarily governed by their sources and size sorting.

4.2. Temporal variations of elemental ratios

It is evident from the above discussions that the geochemistry of the SK187/PC33 sediments effectively preserves the signature of their provenances and their relative variations in the past. Temporal variations in the sediment sources to the studied location can be examined through changes in Al-normalized elemental ratios of the sediments. Figure 5 shows the depth profile of Al-normalized ratios of K, Ti, Cu and Cr, along with the Ti/Ca ratio and CIA of the SK187/PC33 sediments. The strategy behind using elemental ratios of these elements to track the provenances lies in the fact that these elements show distinctly different signatures for the Himalayan (Ganga-Brahmaputra) and the peninsular Indian (Godavari-Krishna) rivers (Table 2). All these elemental ratios show wide variations with the depth of SK187/PC33 core, confirming a change in their provenances in the past. For example, the K/Al varies from 0.22 to 0.37 in the sediment core, which is intermediate to average K/Al ratios of the Ganga (0.29), Brahmaputra (0.33) and the GK (0.21) river system (Table 2). Besides minor excursions, the K/Al ratios of the sediments corresponding to the LGM show systematic lower values (Fig. 5). The lower K/Al ratios during LGM (Fig. 5) possibly indicate relatively decrease in sediment supply from the Himalayan rivers which have characteristically lower K/Al ratios compared to GK rivers. A decline in sediment supply from the Himalayan rivers during the LGM is also evident from the

relatively higher ratios of Ti/Al in the BoB sediments corresponding to the LGM. The Ti/Al ratios of the Ganga (0.06) and Brahmaputra (0.05) river sediments are lower compared to that of the GK river sediments (0.1). Relatively higher Cr/Al and Cu/Al ratios of the SK187/PC33 sediments during this climatic event (Fig. 5) brings also support for reduced Himalayan sediment contribution during the LGM. The Cu/Al and Cr/Al ratios for the Ganga (5 and 12) and Brahmaputra (4 and 13) river sediments are lower compared to that of the GK river sediments (11 and 16). Therefore, the depth profile of K/Al, Ti/Al, Cu/Al and Cr/Al for the SK187/PC33 core consistently indicates that relative sediment supply from the Himalaya reduced during the last glacial maxima (Fig. 5). This conclusion is also consistent with the results of Tripathy et al. (2011a), which based on Sr-Nd isotopes of sediments from the western BoB indicated lowering of sediment supply from the Himalaya during LGM.

Depth profile of Ti/Ca ratio for the SK187/PC33 core showed an interesting shift towards higher values during the Holocene (Fig. 5). Ti in marine sediments mainly comes from detrital sources, whereas Ca in sediments depends on its contributions from detrital and biogenic supply and therefore, Ti/Ca ratio can be used as a proxy to assess the temporal changes in the amount of sediment supply from the continents with respect to that from the biogenic contributions. Further, Ti/Ca ratio can also represent the chemical weathering intensity in the continents as Ti is an immobile element, unlike the Ca which resides in easily weatherable minerals. Therefore, the increase in Ti/Ca ratio during the Holocene (Fig. 5) can be either due to significant increase in detrital supply, or significant increase in chemical weathering intensity. The observed increasing trend in Ti/Ca ratio during the Holocene shows consistency with the trend of CIA for the BoB sediments (Fig. 5). This consistency in trends between CIA, a chemical weathering index and Ti/Ca ratio points enhanced chemical weathering during the Holocene. This increase in chemical weathering for the last ~10 ka could be due to strengthening of monsoon during the Holocene (Goodbred and Kuehl, 2000), which in turn likely to elevate the weathering intensity in the continents. Along with appreciable changes during the LGM, the K/Al ratios in the BoB sediments show a decreasing trend during the Holocene (Fig. 5). This relatively lower K/Al ratio during the Holocene could have resulted from preferential mobilization of K, bringing more support to the proposition of intense chemical weathering during this period.

4.3. Quantification of source contributions using an inverse model

Efforts are made in this study to quantify the contribution from the major provenances for the SK187/PC33 sediments using an inverse model. Inverse modeling of geochemical dataset (Tripathy and Singh, 2010) iteratively solves a set of mass balance equation starting from pre-assigned elemental ratios for the sources and it provides the relative contribution from each of the sources to the core site. It is prerequisite for the model that the elements used in the mass balance equations to estimate the contribution of sediments from the continental sources are mainly from detrital sources and hence, only those elements (*viz.* Al, Fe, Ti, Cr, Co, Cu and V) with higher (> 0.80) factor loading in *Factor 1* (Table 3) are used in this model.

The mass balance equation for an element (*X*) in the BoB sediment can be written as:

$$X = \sum_{i=1}^3 (X_i \times f_i) \quad \text{----- (1)}$$

$$\text{and } \sum_{i=1}^3 (f_i) = 1 \quad \text{----- (2)}$$

where, X_i represents for the elemental concentration of source i and $i = 1, 2,$ and 3 stands for the Ganga, Brahmaputra and the GK rivers respectively. f_i is the fractional contribution of sediments to the core site from the source i .

For Al-normalized ratios of X , Eq. (1) can be re-written as,

$$\left(\frac{X}{Al}\right) \times Al = \sum_{i=1}^3 \left(\left(\frac{X}{Al}\right)_i \times Al_i \times f_i \right) \quad \text{----- (3)}$$

As concentrations of Al for all the three sources (Table 2) are same, Eq. (3) can be reduced to,

$$\left(\frac{X}{Al}\right) = \sum_{i=1}^3 \left(\left(\frac{X}{Al}\right)_i \times f_i \right) \quad \text{----- (4)}$$

Eq. (2) and Eq. (4) for elements $X = \text{Fe, Ti, Cr, Co, Cu}$ and V are used in the inverse model to estimate the source contributions. The a-priori composition for the three sources is listed in the Table (2). The

optimization method used in the inverse model for this study is the same used by Tripathy and Singh (2010).

The estimated sediment contribution from the Ganga, Brahmaputra and the GK rivers to the core site are provided in Table 5. On average, the Himalayan rivers supply $66 \pm 13\%$ of sediments to the core site with $35 \pm 16\%$ alone coming from the Ganga. The GK river supply $34 \pm 13\%$ sediment to the SK187/PC33 core site. These estimates are consistent with that estimated earlier (Tripathy et al., 2011a) using the Sr-Nd isotopic composition of these sediments. The depth profile of sediment contributions from the Himalayan rivers to the SK187/PC33 core site showed large variability (Fig. 6). The combined sediment supply from the Ganga and Brahmaputra is observed to be significant lower during the LGM compared to the range observed during Pre-LGM period. The contribution from the Himalayan rivers reduced from $\sim 70\%$ during Pre-LGM to $\sim 50\%$ during the LGM. This decline trend is also noticed in case of the Ganga; however, it is interesting to note that the sediment contribution from the Brahmaputra remained nearly similar during the LGM and the Pre-LGM period (Fig. 6).

Results from the inverse model show about 20% decline in the sediment contribution from the Himalayan rivers, mainly the Ganga, to the BoB during the LGM. The possible cause for this change in the Himalayan erosion during this climate event could be due to weakening of southwest monsoon (Duplessey, 1982) and the larger glacial extent (Owen et al., 2002) over the HH. Presently, the sediment load of the Himalayan rivers are by and large regulated by the south west monsoon. It has been well documented that the intensity of the SW monsoon relatively decreased during the LGM (Duplessey, 1982; Prell and Kutzbach, 1987; Sarkar et al., 1990). Therefore, it is likely that the relative supply from the Himalaya from the BoB could have decreased in response to weakening of south-west monsoon. Along with the SW monsoon, the river basins in the Brahmaputra and the peninsular India also receive rainfall during north-east monsoon. Hence, the sediment supply from these (Brahmaputra and GK) river basins showed minimal change during the LGM. Furthermore, the extent of glacial cover over the HH (Owen et al., 2002) was higher during LGM due to its high elevation which reduces the exposed area for weathering. The HH is the dominant sediment supplier from the Himalaya to the BoB and hence, larger glacial cover over this geological unit is likely to lower the supply of sediment from the Himalaya to the Bay of Bengal. Observations from this study confirm that the Himalayan erosion is significantly regulated by the changes in the regional climate, hinting towards a climate-erosion link. This conclusion of climate-erosion link is consistent with results from some of the earlier studies on the palaeo-erosion

pattern of the Himalaya (Goodbred, 2003; Ahmad et al., 2005; Kessarkar et al., 2005; Clift et al., 2008; Rahaman et al., 2009; Prakashbabu et al., 2010; Tripathy et al., 2011a). However, these outcomes on linkage of erosion with climate are not concurrent with some of existing studies (Colin et al., 1999; Pierson-Wickmann et al., 2001; Kessarkar et al., 2003; Galy et al., 2008; Goswami et al., 2012) that show insignificant changes in the provenances despite climatic changes during last few ka. The possible reason for this difference is unclear; one possible explanation could be that the studies showing no erosion-climate link are primarily from locations that receive sediments from limited sources and hence, change in erosion pattern in response to climatic changes may not be appreciated in these locations as the geochemical proxies only preserve signatures of relative changes in sources.

Along with the major excursion during the LGM, the estimated sediment contribution from the Ganga is noticed to fall steadily during the Holocene (Fig. 6). The observed reduction in the sediment supply from the Ganga during the Holocene is not consistent with their corresponding Sr-Nd isotopic composition (Tripathy et al., 2011a), which are relatively more robust proxies to trace the sediment provenances (Tripathy et al., 2011b). Further, it has been documented that the monsoon intensity got strengthened during the Holocene, which again rules out possibility of decline in sediment contribution from the Ganga during this period. Therefore, this estimated sediment contribution from the Ganga during the Holocene can be attributable to non-fulfillment of an assumption of the inverse model. Inverse model assumes that the chemical composition of sources remained unchanged during the entire-span of the sediment record. The iteration of the inverse model starts from the pre-assigned input of elemental ratios for various sources and provides the best-fit for most of these samples and their chemical composition. The inverse model was successful in constraining the sediment contribution for most of the samples deposited till the Holocene as these estimates mimic the observed trends of elemental ratios (Fig. 5) and are consistent with the estimates from the Sr-Nd isotopes (Tripathy et al., 2011a). Therefore, the declining trend in the Ganga during the Holocene hints a change in chemical composition of sediment provenances during this period. This change in chemical composition of sediment provenance could have resulted from intense chemical weathering in the river basins during this period, as inferred from the depth profiles of Ti/Ca, CIA and K/Al (Fig. 5).

5. Conclusions

This study investigated the major and trace elemental geochemistry of sediments from a ~13-m long piston core (SK187/PC33) from the western BoB to track the temporal changes in their sediment provenances. Factor analysis of geochemical composition of these sediments indicated that their geochemistry is mainly controlled from their detrital sources, *viz.* sediments derived by the Himalayan and the peninsular Indian rivers. Depth profiles of Al-normalized elemental ratios and the inverse model calculation of these ratios indicated ~20% reduction in the sediment supply from the Himalaya during the LGM. This reduction in sediment supply from the Himalaya is due to weakening of south-west monsoon and large glacial extent over the HH during this climatic event. Results from this study also points to intense chemical weathering in the river basins as a response to strengthened monsoon during the Holocene. These inferences establish a strong link between climate and the Himalayan erosion in a ka timescales.

Acknowledgement

Discussions with S. Krishnaswami and M. M. Sarin during this work are thankfully acknowledged. Thanks to Ravi Bhushan for his help during the carbon and nitrogen analyses.. We thank the Editor and two anonymous reviewers for their constructive suggestions. Financial assistance under the BENFAN project by the Ministry of Earth Sciences, India is highly appreciated. This is NIO contribution No. xxxx.

References

- Ahmad, S. M., Anil Babu, G., Padmakumari, V. M., Dayal, A. M., Sukhija B. S., Nagabhushanam, P., 2005. Sr, Nd isotopic evidence of terrigenous flux variations in the Bay of Bengal: Implications of monsoons during the last ~34,000 years. *Geophys. Res. Lett.* 32, 1-4.
- Aucour, A., France-Lanord, C., Pedroja, K., Pierson-Wickmann, A.-C., Sheppard, S.M.F., 2006. Fluxes and sources of particulate organic carbon in the Ganga-Brahmaputra river system. *Global Biogeochem Cy.*, 20(2): doi:10.1029/2004GB002324.
- Bhushan, R., Dutta, K., Somayajulu, B.L.K., 2001. Concentrations and burial fluxes of organic and inorganic carbon on the eastern margins of the Arabian Sea. *Mar. Geol.*, 178, 95-113.
- Bouchez, J., Gaillardet, J., France-Lanord, C., Maurice, L., Dutra-Maia, P., 2011, Grain size control of river suspended sediment geochemistry: Clues from Amazon river depth profiles. *Geochem. Geophys. Geosyst.*, 12, Q03008, 1-24.

- Braun, J., Descloitres, M., Riotte, J., Fleury, S., Barbiero, L., Boeglin, J., Violette, A., Lacarce, E., Ruiz, L., Sekhar, M., Mohan Kumar, M., Subramanian, S., Dupre, B., 2009. Regolith mass balance inferred from combined mineralogical, geochemical and geophysical studies: Mule Hole gneissic watershed, South India. *Geochim. Cosmochim. Acta*, 73, 935-961.
- Chakrapani, G.J., Saini, R., 2009. Temporal and spatial variations in water discharge and sediment load in the Alaknanda and Bhagirathi Rivers in Himalaya, India. *J. Asian Earth Sci.* 35 545-553.
- Clift, P. D., Giosan, L., Blusztajn, J., Campbell, I. H., Allen, C., Pringle, M., Tabrez, A. R., Danish, M., Rabbani, M. M., Alizai, C. A., Lückge, A., 2008. Holocene erosion of the Lesser Himalaya triggered by intensified summer monsoon. *Geology*, 36, 79-82.
- Colin, C., Turpin, L., Bertaux, J., Desprairies, A., Kissel, C., 1999. Erosional history of the Himalayan and Burman ranges during the last two glacial-interglacial cycles. *Earth Planet. Sci. Lett.*, 171, 647-660.
- Colin, C., Turpin, L., Blamart, D., Frank, N., Kisel, C., Duchamp, S., 2006. Evolution of weathering patterns in the Indo-Burman Ranges over 280 kyr: Effects of sediment provenance on $^{87}\text{Sr}/^{86}\text{Sr}$ ratios tracer. *Geochem. Geophys. Geosyst.*, 7, doi:10.1029/2005GC000962.
- Das, A., Krishnaswami, S., 2007. Elemental geochemistry of river sediments from the Deccan Traps, India: Implications to source of elements and their mobility during basalt-water interaction. *Chem. Geol.* 242, 232-254.
- Duplessy, J.C., 1982. Glacial to interglacial contrasts in the northern Indian Ocean. *Nature*, 295, 494-498.
- France-Lanord, C., Derry, L., Michard, A., 1993. Evolution of the Himalaya since Miocene time: Isotopic and sedimentologic evidence from the Bengal Fan. *Himalayan Tectonics* (Eds. Treloar, P. J. and Searle, M.), *Geol. Soc. Spec. Publ.* 74, 603-621.
- France-Lanord, C., Derry, L., 1997. Organic carbon burial forcing of the carbon cycle from Himalayan erosion. *Nature*, 390, 65-67. (NOT CITED IN TEXT)
- Galy, A., France-Lanord, C., 2001. Higher erosion rates in the Himalaya: Geochemical constraints on riverine fluxes. *Geology*, 29, 23-26.
- Galy, V., Francois, L., France-Lanord, C., Faure, P., Kudrass, H., Palhol, F., Singh, S. K., 2008. C4 plants decline in the Himalayan basin since the Last Glacial Maximum, *Quat. Sci. Rev.*, 27, 1396-1409.
- Garzanti, E., Ando, S., France-Lanord, C., Censi, P., Vignola, P., Galy, V., and Lupker, M., 2011. Mineralogical and chemical variability of fluvial sediments 2. Suspended-load silt (Ganga-Brahmaputra, Bangladesh). *Earth Planet. Sci. Lett.*, 302, 107-120.
- Goodbred, S. L., 2003. Response of the Ganges dispersal system to climate change: a source-to-sink view since the last interstade., *Sediment. Geol.*, 162, 83-104.
- Goodbred, S. L., Kuehl, S., A., 2000. Enormous Ganges-Brahmaputra sediment discharge during strengthened early Holocene monsoon. *Geology*, 28, 1083-1086.

- Goswami, V., Singh, S. K., Bhushan, R., Rai, V. K., 2012. Temporal variations in $^{87}\text{Sr}/^{86}\text{Sr}$ and ϵ_{Nd} in sediments of the southeastern Arabian Sea: Impact of monsoon and surface water circulation. *Geochem. Geophys. Geosyst.*, 13, Q01001, DOI:10.1029/2011GC03802.
- Gupta, L., Subramanian, V., Ittekkot, V., 1997. Biogeochemistry of particulate organic matter transported by the Godavari river, India. *Biogeochemistry*, 38, 2, 103-128.
- Horowitz, A., and Elrick, K., 1987. The relation of stream sediment surface area, grain size and composition to trace element geochemistry. *Appl. Geochem.*, 2, 437-451.
- Huang, S., Conte, M., 2009. Source/process apportionment of major and trace elements in sinking particles in the Sargasso sea. *Geochim. Cosmochim. Acta*, 73, 65-90.
- Islam, M. R., Begum, S. F., Yamaguchi, Y., Ogawa, K., 1999. The Ganges and Brahmaputra rivers in Bangladesh: Basin denudation and sedimentation. *Hydrol. Proc.*, 13, 2907-2923.
- Kessarkar, P. M., Rao, V. P., Ahmad, S. M., Patil, S. K., Anil Kumar, A., Anil Babu, G., Chakraborty, S., Soundar Rajan, R., 2005. Changing sedimentary environment during the Late Quaternary: Sedimentological and isotopic evidence from the distal Bengal Fan, *Deep Sea Res.*, 52, 1591-1615.
- Kessarkar, P. M., Rao, V. P., Ahmad, S. M., Anil Babu G., 2003. Clay minerals and Sr-Nd isotopes of the sediments along the western margin of India and their implication for sediment provenance, *Mar. Geol.*, 202, 55-69.
- Krishnaswami, S., and Tripathy, G. R., 2012. Chemical and Physical erosion of river basins of India: Links to climate and tectonics, *Proc. Indian Natn. Sci. Acad.*, 78, 299-311.
- Lupker, M., France-Lanord, C., Galy, V., Lave, J., Gaillardet, J., Gajurel, A., Guilmette, C., Rahman, M., Singh, S. K., Sinha, R., 2012. Predominant floodplain over mountain weathering of Himalayan sediments (Ganga basin). *Geochim. Cosmochim. Acta*, 84, 410-432.
- Milliman, J. D., 2001. River Inputs. *Encyclopedia of ocean sciences*, 2419-2427.
- Milliman, J. D., Syvitski J., 1992. Geomorphic/tectonic control of sediment discharge of sediment discharge to ocean: the importance of small mountainous rivers. *J. Geol.*, 100, 525-544.
- Nesbitt, H., Young, G., 1982. Early Proterozoic climates and plate motions inferred from major element chemistry of lutites. *Nature*, 299, 715-717.
- Owen, L., Finkel, R., Caffee, M., 2002. A note on the extent of glaciation throughout the Himalaya during the global Last Glacial Maximum. *Quaternary Sci. Rev.*, 21, 147-157
- Panda, D., Kumar, A., Mohanty, S., 2011. Recent trends in sediment load of the tropical (Peninsular) river basins of India. *Global Planet. Change*, 75, 108-118.
- Pattan, J.N., Parthiban, G., Prakashbabu, C., Khadge, N., 2008. A note on geochemistry of surface sediments from Krishna-Godavari basin, East coast of India. *J. Geol. Soc. India*. 71, 107-114.

- Pierson-Wickmann, A., Resiberg, L., France-Lanord, C., 2001., Os-Sr-Nd results from sediments in the Bay of Bengal: Implications for sediment transport and the marine Os record. *Paleoceanography*, 16, 435-444.
- Prakashbabu, C., Pattan, J., Dutta, K., Basavaiah, N., Ravi Prasad, G., Ray, D. K., Govil, P., 2010. Shift in detrital sedimentation in the eastern Bay of Bengal during the late quaternary. *J. Earth Syst. Sci.* 119, 285-295.
- Prell, W. L., Kutzbach, J. E., 1987. Monsoon variability over the past 150, 000 years, *J. Geophys. Res.*, 92, 8411-8425.
- Rahaman, W., Singh, S. K., Sinha, R., Tandon, S. K., 2009. Climate control on erosion distribution over the Himalaya during the past ~100 ka. *Geology*, 37, 559-562.
- Rai, S. K., 2008. Isotopic and Geochemical studies of ancient and modern sediments. Ph.D. Thesis. MS University, Vadodara, 195 pp.
- Sarin, M. M., Borole, D. V., Krishnaswami, S., 1979. Geochemistry and geochronology of sediments from the Bay of Bengal and the equatorial Indian Ocean. *Proc. Indian Acad. Sci.*, 88 A, 131-154.
- Sarkar, A., Ramesh, R., Bhattacharya, S. K., Rajagopalan, G., 1990. Oxygen isotope evidence for a stronger winter monsoon current during the last glaciation. *Nature*, 343, 549-551.
- Singh, S. K., France-Lanord, C., 2002. Tracing the distribution of erosion in the Brahmaputra watershed from isotopic compositions of stream sediments. *Earth Planet. Sci. Lett.*, 202, 645-662.
- Singh, S. K., Rai, S. K., Krishnaswami, S., 2008. Sr and Nd isotopes in river sediments from the Ganga basin: Sediment provenance and spatial variability in physical erosion. *J. Geophys. Res.*, 113, F03006, doi:10.1029/2007JF000909.
- Subramanian, V., Van t' Dack, L., Grieken, R. V., 1985. Chemical composition of river sediments from the Indian Sub-continent. *Chem. Geol.*, 48, 271-279. (NOT CITED IN TEXT)
- Subramanian et al., 2006 ?
- Tiwari, M., Ramesh, R., Somayajulu, B. L. K., Jull, A. J. T., Burr, G. S., 2005. Early deglacial (~19-17 ka) strengthening of the northeast monsoon. *Geophys. Res. Lett.*, 32, 1-4.
- Tripathy, G. R., Singh, S. K., 2010. Chemical erosion rates of river basins of the Ganga system in the Himalaya: Reanalysis based on inversion of dissolved major ions, Sr, and ⁸⁷Sr/⁸⁶Sr. *Geochem. Geophys. Geosyst.*, 11, Q03013, doi: 10.1029/2009GC002862.
- Tripathy, G. R., Singh, S. K., Bhushan, R., Ramaswamy, V., 2011a. Sr-Nd isotope composition of the Bay of Bengal sediments: Impact of climate on erosion in the Himalaya. *Geochem. J.* 45, 175-186.
- Tripathy, G. R., Singh, S. K., Krishnaswami, S., 2011b. Sr and Nd isotopes as tracers of chemical and physical erosion. In: *Handbook of environmental isotope geochemistry*, Ed. M. Baskaran, Springer-Verlag, 521-551, DOI: 10.1007/978-3-642-10637-8_26.

Figure Captions

Figure 1: Location of the sediment core SK187/PC33 in the western BoB. The possible geological units that can supply sediment to this location are also shown.

Figure 2: Depth profile of carbonate, C_{org} , N and C_{org}/N of the sediments of SK187/PC33. Two outliers are not considered here (see text).

Figure 3: Strong correlation of Al with other major and trace elemental composition of sediments from the SK187/PC33 core indicates their dominant supply from detrital sources.

Figure 4: A-CN-K ($Al_2O_3-CaO^*+Na_2O-K_2O$) diagram of the sediments from the SK187/PC33 core. The possible geological units that supply sediment to the studied location are also shown.

Figure 5: Depth profiles of Al-normalized ratios of K, Ti, Cr and Cu of the SK187/PC33 sediments. Downcore variation in Ti/Ca and CIA is also shown. Systematic change in these elemental ratios during LGM indicates that their provenance have varied with reduced sediment supply from the Himalayan rivers during this climatic event. Two anomalous samples are not considered in this depth profile. The straight line in the figure indicates the 3-point moving average of the datasets.

Figure 6: Estimated sediment contributions from the Himalayan rivers to the core site of SK187/PC33 using an inverse model. The grey box in the figure represents the range ($Mean \pm 1\sigma$) observed for sediment contribution before the LGM.

Table 1: Major and trace elemental composition of sediments from the SK187/PC33 core.

SampleID	Na	K	Ca	Mg	Al*	Fe*	Ti	Ba	Cr	Mn	Sr	Co	Cu	Ni	Zn	V*
	(Wt %)							(µg/g)								
<i>10-12cm</i>	1.14	1.95	0.97	1.93	8.96	6.54	0.57	358	117	10946	97	32	66	75	152	130
<i>18-20cm</i>	1.05	2.19	1.37	1.29	7.44	4.05	0.56	407	96	1190	111	21	31	48	140	90
<i>28-30cm</i>	1.12	2.2	1.16	1.98	8.83	6.42	0.57	401	117	1400	105	30	62	69	156	125
<i>109-111cm</i>	1.03	2.14	0.74	1.64	7.95	6.22	0.55	385	124	1727	93	32	70	89	130	119
<i>149-151cm</i>	1.13	2.43	0.87	1.8	8.85	5.63	0.55	461	120	1351	105	27	57	77	120	115
<i>201-203cm</i>	1.08	2.49	1.96	1.69	8.47	4.88	0.45	449	109	856	133	22	45	61	138	106
<i>221-223cm</i>	0.54	1.07	22.7	1.15	2.5	2.17	0.37	239	35	2361	2749	16	8	32	56	30
<i>249-251cm</i>	1.16	2.33	1.64	1.8	8.82	5.78	0.5	559	110	977	133	26	66	79	132	112
<i>300-302cm</i>	0.97	1.99	2.31	1.62	7.89	5.57	0.45	533	103	1014	150	26	59	78	124	108
<i>320-322cm</i>	1.1	1.88	13.4	2.59	6.28	3.97	0.34	363	85	1685	531	23	36	68	397	77
<i>350-352cm</i>	1.29	2.7	7.48	3.37	8.63	4.69	0.38	365	86	1689	500	22	44	63	546	78
<i>400-402cm</i>	1.36	2.07	10.75	2.68	6.41	3.87	0.36	520	95	1572	186	24	40	79	461	78
<i>440-442cm</i>	0.74	1.03	29.4	1.62	2.84	1.84	0.16	231	37	3111	4159	10	16	28	250	34
<i>450-452cm</i>	0.99	2.43	4.25	1.66	8.27	4.97	0.44	383	102	1648	262	25	44	68	104	105
<i>500-502cm</i>	1.02	3.08	2.75	1.94	8.22	4.47	0.5	463	89	941	123	25	36	64	99	99
<i>550-552cm</i>	1.68	2.03	6.11	2.1	6.15	2.52	0.27	365	60	662	213	16	16	39	333	49
<i>600-602cm</i>	1.42	2.04	11.5	3.36	6.8	4.42	0.5	409	107	1589	434	26	41	70	545	104
<i>650-652cm</i>	0.97	2.01	6.24	2.11	7.3	4.88	0.41	551	90	2543	318	33	56	87	188	115
<i>700-702cm</i>	1.1	2.15	4.62	2.11	7.77	4.84	0.48	489	88	1782	233	33	53	79	158	112
<i>750-752cm</i>	1.46	2.4	2.87	1.7	7.75	3.84	0.38	429	67	1440	173	21	27	45	110	83
<i>800-802cm</i>	1.35	2.42	8.12	3.39	8.13	4.86	0.31	406	103	1926	254	29	40	77	467	89
<i>849-851cm</i>	1.11	2.05	2.92	1.54	6.81	3.57	0.4	401	71	1765	187	21	25	46	144	79
<i>899-901cm</i>	1.02	1.69	16.22	2.6	5.57	3.69	0.29	365	66	1396	886	24	37	62	418	56
<i>949-951cm</i>	1.06	2.52	2.59	1.78	7.87	4.82	0.39	497	84	1217	150	33	44	68	114	103
<i>999-1001cm</i>	0.84	1.57	4.79	1.7	4.55	2.63	0.21	338	50	1096	170	15	27	38	278	53
<i>1049-1051cm</i>	1.16	2.67	2.6	1.7	8.07	4.46	0.38	437	77	883	144	22	37	43	97	94
<i>1099-1101cm</i>	1.18	3.03	2.4	1.85	8.72	4.98	0.43	487	83	1026	153	24	41	53	109	103
<i>1149-1151cm</i>	1.65	2.61	2.25	1.45	7.55	3.68	0.42	409	61	615	147	19	24	37	83	73
<i>1199-1201cm</i>	2.39	1.97	1.89	0.8	6	1.86	0.22	340	26	284	156	9	7	15	93	35
<i>1219-1221cm</i>	1.06	2.72	2.25	1.94	9.19	4.87	0.43	434	83	753	123	22	42	47	160	96

*Al, Fe and V data are from Tripathy et al. (2011a)

Table 2: Comparison of average chemical compositions ($\pm 1\sigma$) of sediments of the SK187/PC33 core with their possible sedimentary sources, *viz.* sediments from the Himalayan (Ganga and Brahamaputra) and peninsular India rivers.

	Ganga ¹	Brahmaputra ¹	Godavari-Krishna ²	SK187/PC33*	
				Total	Carbonate-corrected [@]
Al	7.9 ± 2.2	8.0 ± 1.1	8.0 ± 0.4	7.3 ± 1.7	8.0 ± 1.2
Fe	4.6 ± 2.0	4.1 ± 0.7	6.4 ± 0.3	4.4 ± 1.3	4.8 ± 1.1
Ti	0.5 ± 0.1	0.4 ± 0.5	0.8 ± 0.1	0.4 ± 0.1	0.5 ± 0.1
Mg (wt%)	1.5 ± 0.5	1.6 ± 0.4	1.5 ± 0.1	2.0 ± 0.6	2.2 ± 0.8
K	2.3 ± 0.5	2.6 ± 0.3	1.7 ± 0.01	2.2 ± 0.5	2.4 ± 0.4
Ca	2.1 ± 1.0	1.4 ± 0.2	2.0 ± 0.3	6.0 ± 6.8	1.9 ± 2.2 ^{&}
Na	0.7 ± 0.3	1.3 ± 0.1	0.6 ± 0.3 ^S	1.2 ± 0.3	1.3 ± 0.3
Ba	448 ± 107	510 ± 51	205 ± 3	416 ± 79	-
V	100 ± 46	93 ± 19	192 ± 23	88 ± 28	97 ± 25
Cr	95 ± 35	102 ± 33	129 ± 13	85 ± 26	94 ± 24
Cu	40 ± 29	32 ± 17	91 ± 20	40 ± 17	44 ± 16
Ni µg/g	47 ± 25	49 ± 19	84 ± 9	59 ± 19	67 ± 20
Zn	90 ± 34	86 ± 20	151 ± 25	210 ± 147	245 ± 184
Sr	88 ± 23	136 ± 19	140 ± 43	439 ± 857	-
Co	15 ± 6	16 ± 4	30 ± 3	24 ± 6	26 ± 6
Mn	908 ± 248	1000	800 ± 100	1715 ± 1843	-

Data Source: ¹Garzanti et al., 2011; ²Pattan et al., 2008; ³Das and Krishnaswami, 2007; *Present Study. [&](Total Ca-Ca from carbonates).

[@]Carbonate-corrected concentrations were calculated assuming insignificant supply of the element from the carbonates.

Table 3: CaCO₃, C_{org} and N concentrations and C_{org}/N ratio of BoB sediments from the SK187/PC33 core.

Depth (cm)	CaCO ₃	C _{org} (wt %)	TN	C _{org} /N	Depth (cm)	CaCO ₃	C _{org} (wt %)	TN	C _{org} /N
2-4	3.3	0.7	0.07	10.0	620-622	9.7	0.6	0.06	10.0
10-12	1.7	1.1	0.12	9.2	630-632	10.4	0.9	0.08	11.3
18-20	1.5	0.8	0.07	11.4	640-642	6.9	0.3	0.03	10.0
28-30	1.1	1	0.08	12.5	650-652	14.1	1.1	0.09	12.2
38-40	2.1	0.8	0.06	13.3	660-662	10.1	1.2	0.12	10.0
48-50	3	0.3	b.d.		670-672	7	0.6	0.05	12.0
58-60	2.4	0.7	0.05	14.0	680-682	11.2	0.8	0.07	11.4
68-70	2.8	0.7	0.07	10.0	690-692	6.1	0.4	0.03	13.3
78-80	3.7	0.5	0.04	12.5	700-702	10.2	0.9	0.09	10.0
89-91	2.2	1.2	0.13	9.2	710-712	6	-	-	-
109-111	1.2	1.3	0.12	10.8	720-722	4.9	0.1	b.d.	-
111-113	1.5	1.5	0.13	11.5	730-732	5.7	-	-	-
121-123	1.1	1.1	0.07	15.7	740-742	8.5	-	-	-
129-131	2.5	0.6	0.05	12.0	750-752	5.9	0.5	0.03	16.7
141-143	1.2	1.1	0.07	15.7	760-762	7.5	-	-	-
149-151	1.5	0.1	0.09	1.1	770-772	16.2	-	-	-
161-163	1.6	1.6	0.42	3.8	780-782	13.7	0.6	0.03	20.0
169-171	1.1	1.4	0.13	10.8	790-792	6.2	-	-	-
181-183	4.9	0.9	0.07	12.9	800-802	8.3	1.1	0.12	9.2
189-191	0.9	1.2	0.12	10.0	810-812	8	-	-	-
201-203	3.8	1.2	0.08	15.0	819-821	6.5	1.3	0.11	11.8
209-211	19.6	0.5	0.06	8.3	829-831	5.2	-	-	-
221-223	50.5	0.3	0.02	15.0	839-841	5.2	-	-	-
229-231	2.2	1.2	0.12	10.0	849-851	5.2	0.6	0.05	12.0
241-243	1.1	0.6	0.11	5.5	859-861	5.3	-	-	-
249-251	3.1	1.3	0.12	10.8	869-871	5.4	-	-	-
260-262	2.9	1.1	0.09	12.2	879-881	6.4	1.5	0.12	12.5
270-272	14.5	0.5	0.04	12.5	889-891	6.9	-	-	-
280-282	2.4	1.2	0.1	12.0	899-901	27.9	-	-	-
290-292	3.9	-	-	-	909-911	7.6	0.3	0.03	10.0
300-302	4.9	1	0.1	10.0	919-921	10.7	0.3	0.03	10.0
310-312	7.7	0.3	0.08	3.8	929-931	4.9	-	-	-
320-322	23	1.1	0.07	15.7	939-941	5.1	-	-	-
330-332	13.9	2.9	0.23	12.6	949-951	5.7	1	0.09	11.1
340-342	6	0.8	0.04	20.0	959-961	11.4	-	-	-
350-352	6	0.5	0.04	12.5	969-971	8.7	-	-	-

360-362	6	1.2	0.07	17.1	979-981	15.6	-	-	-
370-372	7.1	0.5	0.05	10.0	989-991	13.1	-	-	-
380-382	7.4	-	-	-	999-1001	7	1.2	0.08	15.0
390-392	6.2	1.5	0.14	10.7	1009-1011	6.7	-	-	-
400-402	13.8	0.8	0.06	13.3	1019-1021	7.3	0.1	0.01	10.0
410-412	5.7	0.6	0.05	12.0	1029-1031	7.3	-	-	-
420-422	6	0.4	0.03	13.3	1039-1041	5.1	-	-	-
430-432	15.9	0.7	0.06	11.7	1049-1051	6.3	0.4	0.03	13.3
440-442	53.9	6.7	0.04	167.5	1059-1061	5.4	-	-	-
450-452	10	1.3	0.11	11.8	1069-1071	5.3	-	-	-
460-462	6.6	0.2	0.02	10.0	1079-1081	6.2	0.6	0.04	15.0
470-472	8.3	1.1	0.09	12.2	1089-1091	5.5	-	-	-
480-482	3	2.1	0.08	26.3	1099-1101	5.6	0.7	0.04	17.5
490-492	2.9	1.7	0.08	21.3	1109-1111	4.8	-	-	-
500-502	7.1	0.6	b.d.	-	1119-1121	5	1	0.08	12.5
510-512	4.5	0.8	0.07	11.4	1129-1131	4.5	-	-	-
520-522	7.3	1.2	0.08	15.0	1139-1141	4.2	-	-	-
530-532	0.2	-	-	-	1149-1151	3.3	0.2	0.03	6.7
540-542	12.9	0.8	0.15	5.3	1159-1161	3.3	-	-	-
550-552	5.2	0.2	b.d.	-	1169-1171	2.6	-	-	-
560-562	7.7	0.9	0.07	12.9	1179-1181	1.6	0.2	-	-
570-572	7.3	-	-	-	1189-1191	1.6	-	-	-
580-582	12.1	1.1	0.06	18.3	1199-1201	1.7	0.2	-	-
590-592	21.6	-	-	-	1209-1211	4	-	-	-
600-602	14.3	0.8	0.21	3.8	1219-1221	3.9	0.6	0.05	12.0
610-612	11.2	0.8	0.06	13.3					

Table 4: Factor analysis of geochemical dataset of the SK187/PC33 core indicates four factors with Eigen values >1. The dominant chemical species of each factor are highlighted in gray.

	Factor 1	Factor 2	Factor 3	Factor 4
Eigen Value	<i>9.0</i>	<i>3.3</i>	<i>2.3</i>	<i>1.5</i>
% Variance	<i>47</i>	<i>17</i>	<i>12</i>	<i>8</i>
Na	0.01	-0.57	0.55	0.19
K	0.68	-0.41	0.30	0.02
Ca	-0.77	0.56	-0.08	0.16
Mg	0.20	0.59	0.56	0.51
Al	0.92	-0.19	0.14	-0.01
Fe	0.93	0.24	-0.14	-0.06
Ti	0.81	0.06	-0.31	-0.12
CaCO₃	-0.76	0.52	-0.26	0.02
Corg	0.21	-0.49	-0.51	0.66
TN	0.21	-0.49	-0.51	0.66
Ba	0.74	-0.11	0.18	-0.07
Cr	0.89	0.30	-0.07	0.10
Mn	0.12	0.40	-0.42	0.09
Sr	-0.76	0.38	-0.40	0.07
Co	0.83	0.42	-0.06	-0.04
Cu	0.86	0.38	-0.14	-0.06
Ni	0.77	0.55	0.01	0.10
Zn	-0.15	0.53	0.62	0.52
V	0.96	0.13	-0.19	-0.01

Table 5: Results from the inverse model on sediment contributions (in %; Errors are in $\pm\sigma$) from the Ganga, Brahmaputra and the Godavari-Krishna river systems to the SK187/PC33 core site.

Sample ID	Ganga	Brahmaputra	GB rivers*	GK rivers
10-12 cm	21 \pm 6	30 \pm 8	51 \pm 10	49 \pm 4
18-20 cm	17 \pm 6	60 \pm 8	77 \pm 10	23 \pm 3
28-30 cm	20 \pm 6	34 \pm 8	54 \pm 10	46 \pm 4
109-111 cm	14 \pm 6	26 \pm 8	40 \pm 10	60 \pm 5
149-151 cm	21 \pm 6	38 \pm 8	61 \pm 10	39 \pm 4
201-203 cm	30 \pm 6	39 \pm 8	69 \pm 10	31 \pm 3
249-251 cm	31 \pm 6	25 \pm 8	56 \pm 10	44 \pm 4
300-302 cm	26 \pm 6	26 \pm 8	52 \pm 10	48 \pm 4
320-322 cm	27 \pm 6	34 \pm 8	61 \pm 10	39 \pm 4
350-352 cm	54 \pm 5	17 \pm 6	71 \pm 8	29 \pm 3
400-402 cm	25 \pm 6	33 \pm 8	59 \pm 10	41 \pm 4
450-452 cm	30 \pm 6	36 \pm 7	66 \pm 10	34 \pm 3
500-502 cm	30 \pm 6	44 \pm 7	74 \pm 9	26 \pm 3
550-552 cm	53 \pm 5	34 \pm 6	87 \pm 8	13 \pm 2
600-602 cm	11 \pm 6	48 \pm 7	59 \pm 9	42 \pm 4
650-652 cm	26 \pm 6	20 \pm 8	46 \pm 10	54 \pm 5
700-702 cm	28 \pm 6	25 \pm 8	53 \pm 10	47 \pm 4
750-752 cm	48 \pm 5	32 \pm 6	80 \pm 8	20 \pm 2
800-802 cm	48 \pm 5	17 \pm 6	66 \pm 8	34 \pm 3
849-851 cm	31 \pm 6	48 \pm 7	79 \pm 9	21 \pm 3
899-901 cm	40 \pm 5	16 \pm 7	56 \pm 9	44 \pm 4
949-951 cm	38 \pm 6	23 \pm 7	61 \pm 9	39 \pm 4
999-1001 cm	43 \pm 5	18 \pm 7	62 \pm 9	38 \pm 4
1049-1051 cm	46 \pm 5	26 \pm 7	72 \pm 8	28 \pm 3
1099-1101 cm	44 \pm 5	27 \pm 7	71 \pm 9	29 \pm 3
1149-1151 cm	49 \pm 5	34 \pm 6	83 \pm 8	17 \pm 2
1199-1201 cm	86 \pm 4	11 \pm 5	97 \pm 6	3 \pm 2
1219-1221 cm	51 \pm 5	23 \pm 6	74 \pm 8	26 \pm 3

**Sum of contributions from the Ganga and the Brahmaputra rivers.*

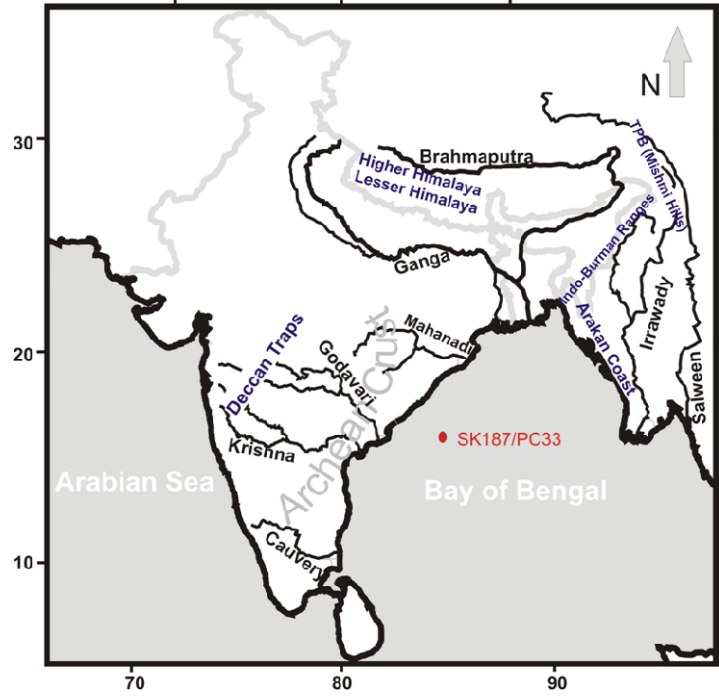


Figure 1

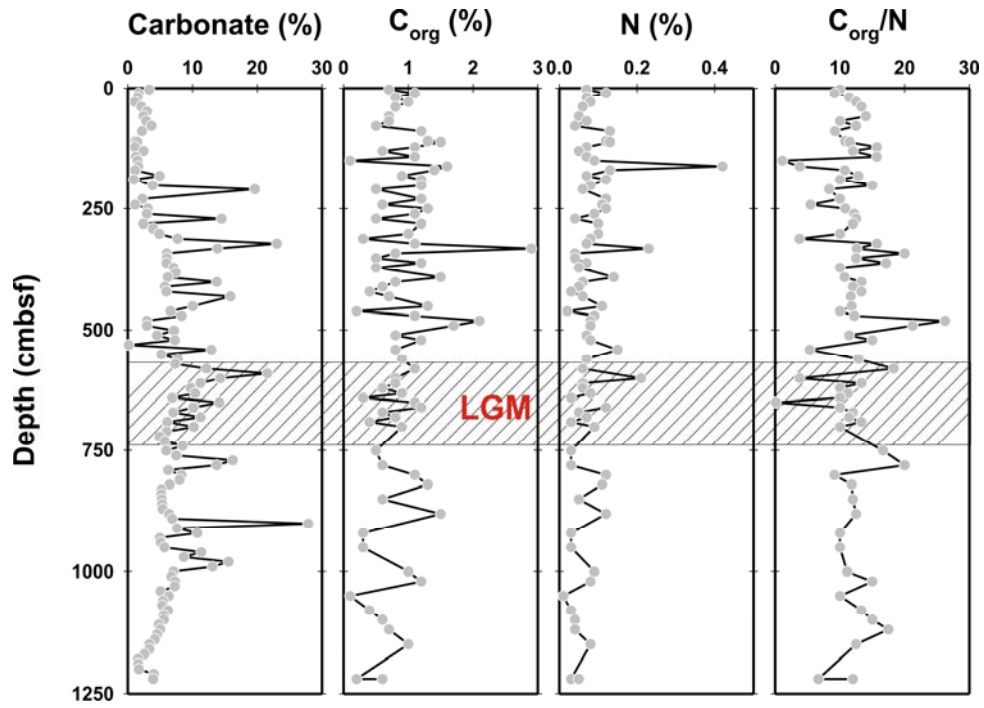


Figure 2

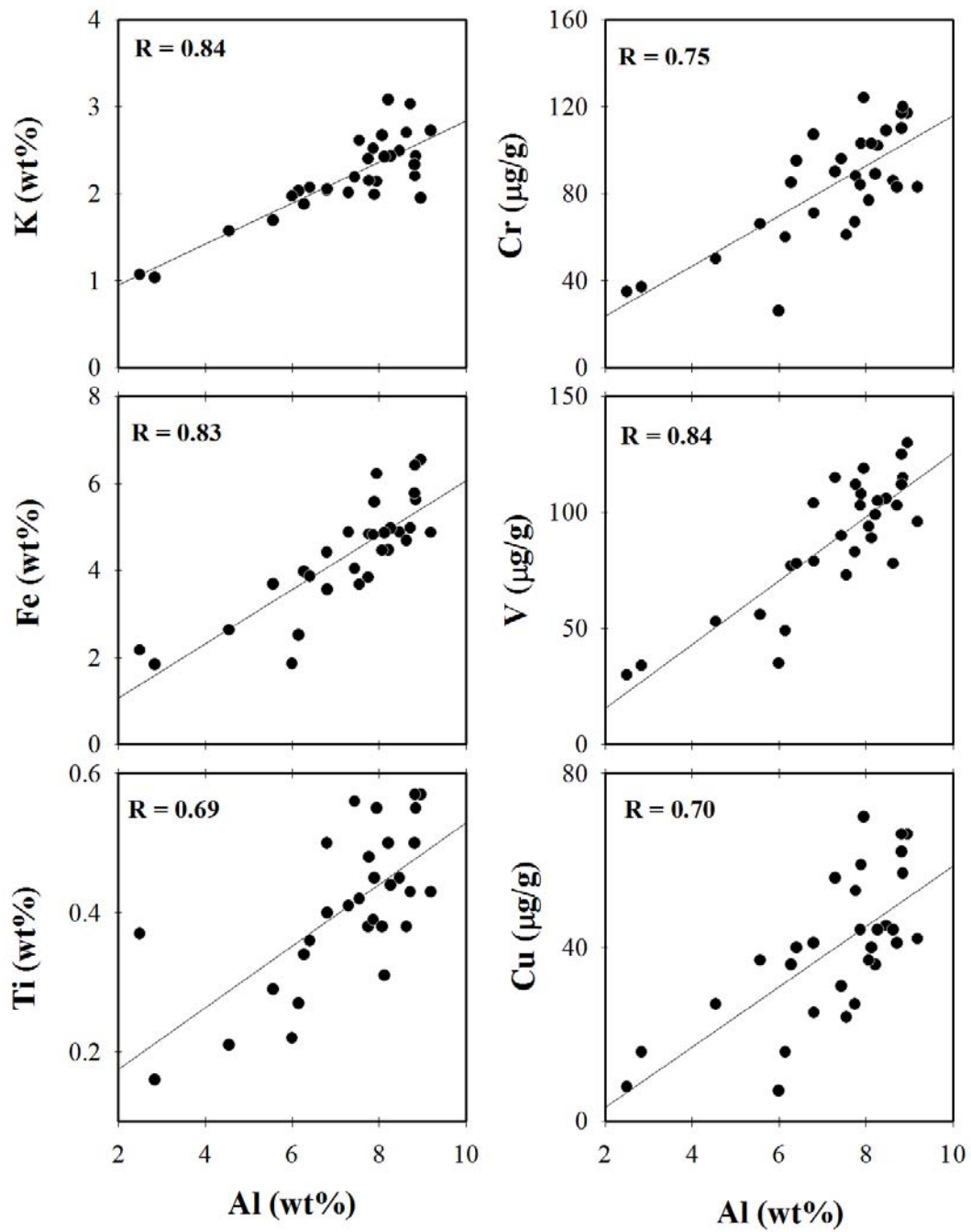


Figure 3

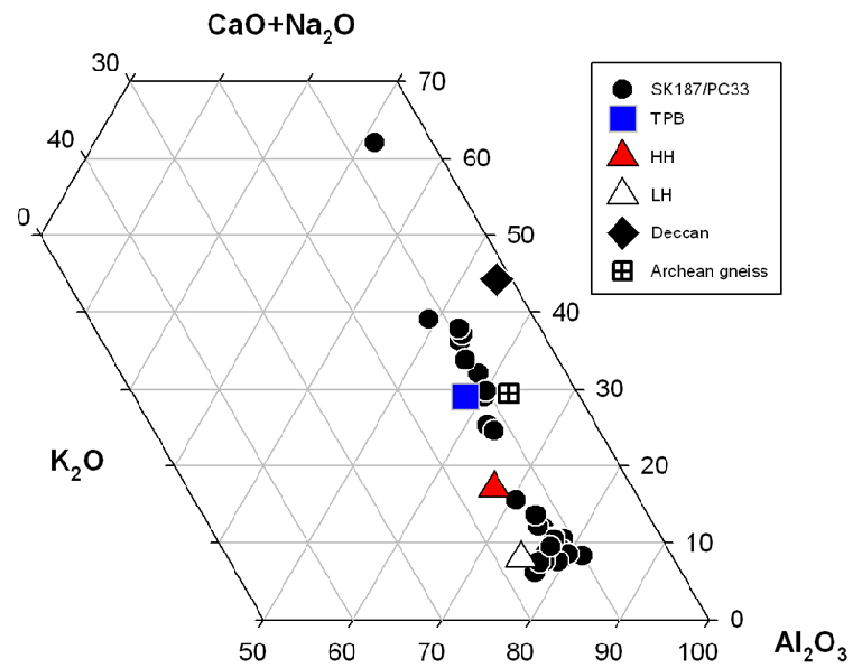


Figure 4

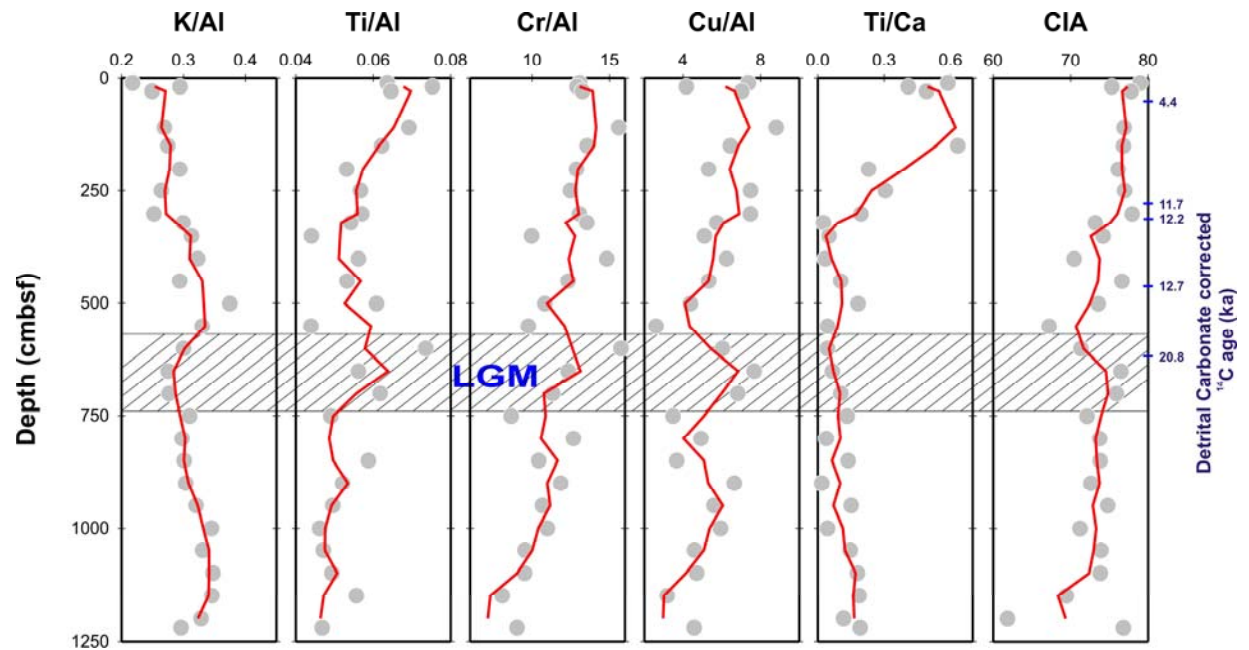


Figure 5

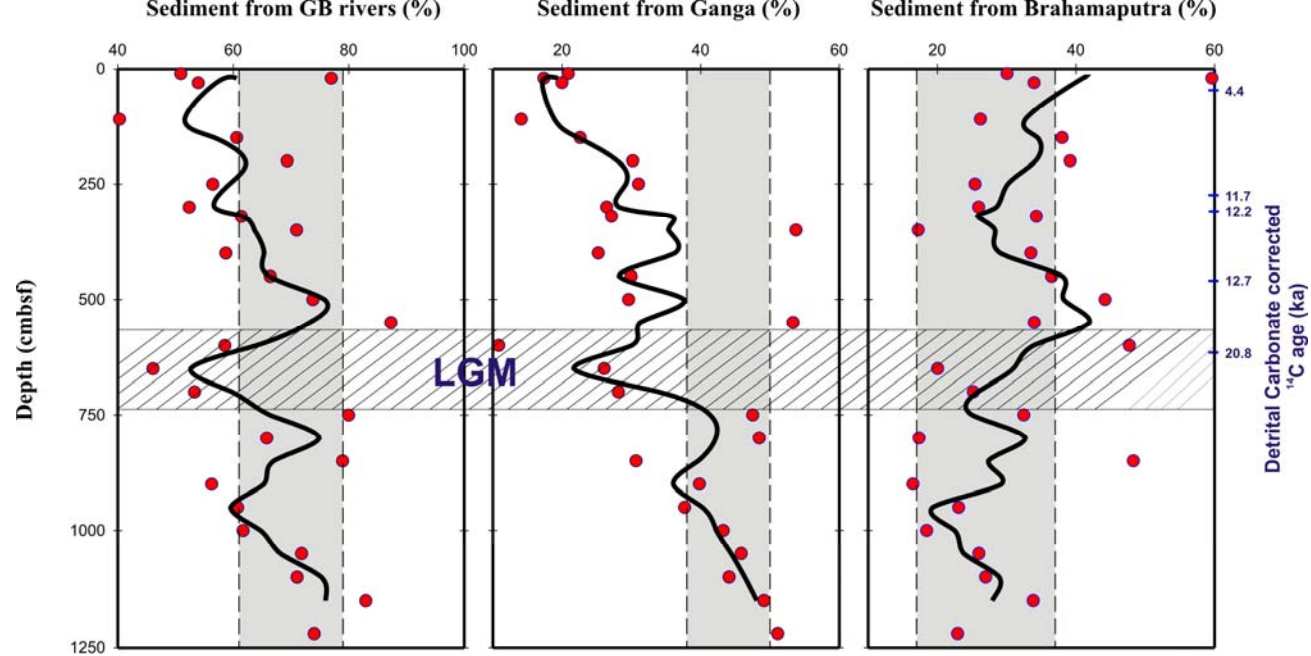


Figure 6